

Aerodynamic Design of Supersonic Cruise Wings with a Calibrated Linearized Theory

Michael J. Mann*

NASA Langley Research Center, Hampton, Virginia 23665

and

Harry W. Carlson†

Lockheed Engineering and Sciences Company, Hampton, Virginia 23666

The design of supersonic cruise wings for minimum drag due to lift is examined in this study. The aerodynamic design method is based on a supersonic linearized theory modified to include corrections for attainable leading-edge thrust and vortex forces. A semiempirical design and estimation method has been developed to account for the deficiencies of the linearized theory which tends to overestimate the required amount of twist and camber and predicts an unattainable level of performance. Comparisons of theoretical and experimental results showed that the semiempirical method provides for the selection of the amount of twist and camber required for maximum performance at cruise and gives a good estimate of the level of performance.

Nomenclature

AR	= aspect ratio, b^2/S
b	= span, in.
C_A	= axial force coefficient
C_D	= drag coefficient
$C_{D,0}$	= drag coefficient at zero lift for a configuration with no twist or camber
C_L	= lift coefficient
$C_{L,cruise}$	= cruise lift coefficient
$C_{L,des}$	= design lift coefficient
$C_{L,\alpha}$	= theoretical lift curve slope at $\alpha = 0$, deg^{-1}
C_m	= pitching moment coefficient
C_N	= normal force coefficient
K_D	= design lift coefficient factor
K_S	= suction parameter factor
M	= Mach number
R	= Reynolds number based on mean aerodynamic chord
S	= reference area, in^2
S_s	= suction parameter
y	= spanwise distance from centerline, in.
α	= angle of attack, deg
α_{des}	= angle of attack corresponding to design lift coefficient, deg
α_{zt}	= angle of attack for zero thrust at a given span station, deg
α_0	= theoretical angle of attack corresponding to zero lift, deg
ΔC_D	= drag coefficient due to lift, $C_D - C_{D,0}$
$\Delta\alpha_{ft}$	= range of angle of attack for full theoretical leading-edge thrust at a given span station, deg

β	= $\sqrt{M^2 - 1}$
Λ_{le}	= leading-edge sweep, deg

Subscripts

des	= design
exp	= experiment
le	= leading edge
max	= maximum
opt	= optimum

Introduction

TRADITIONAL supersonic design and analysis methods are based on linear theory.¹ Advanced computational methods based on the Euler or Navier-Stokes equations are currently under development and offer the promise of greater accuracy than the linearized methods.² However, modified linearized theory provides a simplified and rapid method for the preliminary design of supersonic wings and slender supersonic aircraft. The modified linear theory method of Ref. 3 can be used for the design and analysis of supersonic wings. This method includes corrections to the basic linearized theory for attainable leading-edge thrust and the forces due to separated leading-edge vortex flow. Even with these corrections, however, the drag predicted by this linear method at supersonic speeds is lower than the experimental values of drag, and the amount of twist and camber called for by the theory is larger than is actually required.

A semiempirical design and estimation method developed in Ref. 4 provides a means for correction of the modified linear theory of Ref. 3. This semiempirical method is based on a correlation of theoretical and experimental results for a number of supersonic wings. The correlation was made for a variety of wing planforms and includes a range of supersonic cruise Mach numbers (1.62–3.5) and design lift coefficients. For a given cruise condition, the semiempirical method determines the appropriate linear theory design lift coefficient and gives a reasonably accurate estimate of the performance which can actually be achieved at the cruise condition. This article provides a description of the semiempirical design and estimation method and gives a few selected examples^{4,5} which illustrate its application to the design of supersonic cruise wings for minimum drag due to lift.

Theoretical Considerations

The modified linear theory computer code (designated WINGDES2³) was used for the calculations of this study. This

Presented as Paper 91-3302 at the AIAA 9th Applied Aerodynamics Conference, Baltimore, MD, Sept. 23–25, 1991; received May 6, 1992; revision received Oct. 2, 1992; accepted for publication Oct. 2, 1992. Copyright © 1991 by the American Institute of Aeronautics and Astronautics, Inc. No copyright is asserted in the United States under Title 17, U.S. Code. The U.S. Government has a royalty-free license to exercise all rights under the copyright claimed herein for Governmental purposes. All other rights are reserved by the copyright owner.

*Aerospace Engineer, Vehicle Integration Branch, Advanced Vehicles Division, MS 412. Member AIAA.

†Aerospace Engineer; currently Advanced Aircraft Branch, Advanced Vehicles Division, NASA Langley Research Center, MS 411, Hampton, VA 23665. Member AIAA.

code provides an estimate of attainable leading-edge thrust and leading-edge vortex forces as well as the forces due to the basic attached flow. The code has both a design and analysis capability. Although a prime goal of this study has been the development of a semiempirical design method, the use of existing experimental data required that the code be used in the analysis mode only.

Drag and Suction Parameter

Aircraft drag at supersonic speeds is mainly composed of wave drag due to thickness or volume, skin friction drag, and drag due to lift. The drag due to lift, composed of wave drag due to lift and vortex drag, is responsible for about half of the total drag at lift coefficients near maximum lift-drag ratio. Hence, minimization of the drag due to lift will have a substantial influence on supersonic performance. This is the drag contribution estimated by the WINGDES2 code.³ The combination of wave drag due to thickness and skin friction drag is assumed to equal $C_{D,0}$, the drag of a configuration without twist or camber at zero lift. Whenever possible, experimental values of $C_{D,0}$ were used in this study.

In comparing the aerodynamic performance of various wing designs, it is convenient to have a common figure of merit. The lift-drag ratio which is often used for this purpose is affected by thickness as well as pure lift effects and is not used here. Because this study concentrates on lifting efficiency, the suction parameter is used for the purpose of rating the performance. The suction parameter is defined by the equation

$$S_s = \frac{C_L \tan(C_L/C_{L,\alpha}) - \Delta C_D}{C_L \tan(C_L/C_{L,\alpha}) - C_L^2/(\pi AR)}$$

With this parameter, the wing drag is compared with upper and lower bounds. The upper bound $C_{D,0} + C_L \tan(C_L/C_{L,\alpha})$ is the drag of a flat wing with no leading-edge thrust and no vortex forces. Actually, flat wings will develop some degree of leading-edge thrust and/or some degree of vortex forces, and will generally have somewhat lower drags than given by the upper limit. The lower bound $C_{D,0} + C_L^2/(\pi AR)$ is the theoretical drag of a wing with an elliptical span load distribution and no supersonic wave drag due to lift. This limit is a carry over from subsonic speeds where the limit is reasonably achievable. The presence of wave drag due to lift at supersonic speeds prevents a close approach to this value. A prime advantage of these upper and lower bounds is their simplicity and repeatability. As shown by the equation, the suction parameter is a measure of the wing's departure from the upper limit and approach to the lower bound.

Leading-Edge Thrust and Vortex Forces

Since the basic attached flow solution does not include the effects of leading-edge thrust or leading-edge vortices, these effects must be taken into account and combined with the attached flow solution. Wing performance is critically dependent upon the development of leading-edge thrust. This thrust occurs when the leading edge is subsonic ($\beta \cot \Lambda_{le} < 1$) and is caused by the flow around the leading edge from a lower surface stagnation point. Theoretically, this is a concentrated force which acts tangent to the wing camber surface at the leading edge. Thus, in the case of a cambered wing, the thrust contributes to both axial and normal forces.

The theoretical leading-edge thrust in the WINGDES2 code is calculated⁶ and the amount of thrust which actually develops is estimated by the attainable thrust method.⁷ The attainable leading-edge thrust prediction is based on the fundamental principle that limitations in the attainable pressure levels and the areas over which they act determine the level of thrust. Simple sweep theory was used⁷ to permit a two-dimensional analysis. A combination of two-dimensional airfoil theory and experimental airfoil data were then used to define the limi-

tations on thrust as a function of wing geometry, Mach number, and Reynolds number.

For wings with sharp leading edges, for which no leading-edge thrust is assumed to develop, Polhamus⁸ established a relationship between the normal force induced by separated vortex flow and the theoretical leading-edge thrust. According to the Polhamus suction analogy, the suction vector is assumed to rotate to a position normal to the wing surface, where it affects the normal force rather than the chord force. For a wing with partial leading-edge thrust estimated by the method of Ref. 7, it is assumed that the undeveloped portion of the theoretical leading-edge thrust is converted to a vortex normal force.

Wing Design with Linear Theory

A series of arrow wings has been used to examine the use of linear theory for the design of wing twist and camber.^{9,10} The wings are members of a family with a leading-edge sweep of 70 deg and an aspect ratio of 2.24. Wings were designed for lift coefficients of 0 (uncambered or flat), 0.08, and 0.16 at a Mach number of 2. The wings have sharp leading edges with streamwise thickness distributions of a 3%-thick circular-arc airfoil. The cambered wings were designed by the methods of Refs. 11 and 12. The design method was used to determine the optimum combination of three candidate loadings which would minimize drag at a given lift coefficient and restrict the leading-edge pressure loading to $1.4C_{L,des}$. The leading-edge loading and sweep angle were selected to avoid transonic shocks and flow separation in the cross plane.

Experimental results for the $C_{L,des} = 0.08$ wing are compared with theoretical predictions of the WINGDES2 code in Fig. 1. The semispan models for the 70-deg arrow wings were tested on a boundary-layer bypass plate which produced a freestream Mach number of 2.05. The WINGDES2 calculation includes attainable leading-edge thrust which was computed using an estimated leading-edge radius of 0.004 in. The axial and normal forces are calculated and plotted as a function of the angle $\alpha - \alpha_0$ where α_0 is the theoretical angle of attack for zero lift. This adjustment to α provides a better comparison of cambered wing axial force results with the theoretical flat wing full leading-edge thrust curve. Both theoretical axial force and suction parameter for the cambered wing agree well with the flat wing full thrust solution near the design condition. This agreement illustrates the use of camber to develop a distributed thrust on the forward portion of the wing as a means of recovering the portion of the concentrated leading-edge thrust which the flat wing cannot develop. The theoretical results of WINGDES2 give a reasonably good

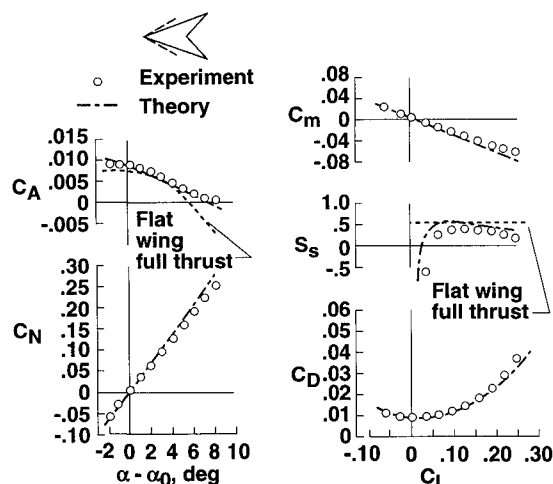


Fig. 1 Comparison of modified linear theory with experimental data for 70-deg swept arrow wing with $C_{L,des} = 0.08$, $M = 2.05$, $R = 4.4 \times 10^6$. Flat wing full thrust curve is for flat wing with theoretical leading-edge thrust.

estimate of the experimental results; however, the theory overestimates the suction parameter and, therefore, underestimates the drag.

The suction parameter can be presented in another format which is particularly useful from the design standpoint. Suction parameter plots for each of the three 70-deg arrow wings (each for a given $C_{L,des}$, e.g., in Fig. 1) were used to develop the curves shown in Fig. 2. Each of the three plots in Fig. 2 shows the variation of suction parameter, at a given lift coefficient, with design lift coefficient. The lift coefficient selected for each plot can be considered to represent $C_{L,cruise}$ so that each plot shows the variation of performance (suction parameter) at some cruise condition with design lift coefficient. Lift coefficients of 0.08, 0.12, and 0.16 were selected and the variation is shown for both theory and experiment. Three data points were used to define each experimental curve, although only two points are shown for $C_L = 0.08$. In every case, both theory and experiment illustrate improvement in performance over the flat wing through the use of some degree of twist and camber as measured by $C_{L,des}$. The theoretical suction parameter peaks at a value of $C_{L,des}$ which is equal to or nearly equal to the selected value of C_L . Thus, the $C_{L,des}$ for maximum theoretical suction parameter, $C_{L,des,opt,theory}$, can be equated to $C_{L,cruise}$. The experimental results show that the suction parameter actually peaks at a lower value of $C_{L,des}$. It turns out that the ratio of the $C_{L,des}$ for the peaks of the theoretical and experimental suction parameters is essentially a constant dependent only on the freestream Mach number. This result will be used in the next section to develop a semiempirical design procedure. This procedure also includes an estimation method which accounts for the fact that the experimental value of maximum suction parameter is lower than the theoretical value as shown in Fig. 2.

The optimum $C_{L,des}$ for the real flow is lower than that given by linearized theory because, as shown in Refs. 4 and 5, the linear theory overestimates the upwash field ahead of the wing. The overestimation of the upwash causes the theory to require too much camber in the leading edge for the proper development of wing leading-edge load and its associated distributed thrust.

Empirical Design Guidelines

Publication of the results for the 70-deg arrow wings⁹ led many supersonic wing designers to apply a "rule of thumb" in which the theoretical design lift coefficient was some fraction (0.5–0.8) of the operating or cruise C_L . An example of this technique is given in Refs. 13 and 14 which describe the development of a NASA supersonic transport configuration

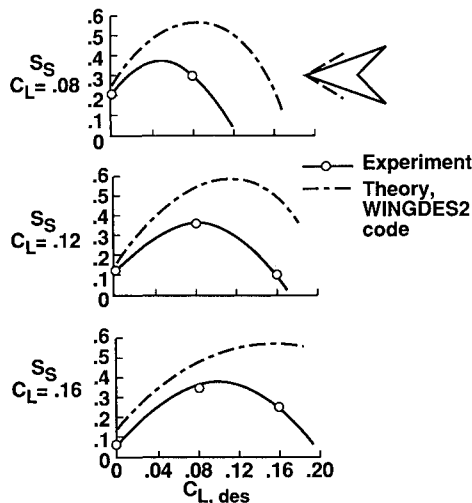


Fig. 2 Variation of suction parameter at three different lift coefficients with design lift coefficient for 70-deg swept arrow wings. $M = 2.05$, $R = 4.4 \times 10^6$.

known as SCAT 15-F. This configuration was used to demonstrate the integration of various design techniques which were being developed at the time. One of the key design techniques was the use of wing twist and camber. In this section a set of guidelines will be developed which attempt to quantify the relationship between the linear theory design lift coefficient and the cruise lift coefficient, and to provide an estimate of the level of performance which can be achieved. The guidelines essentially lead to a semiempirical method for the design of supersonic wings with minimum drag due to lift.

Derivation of a Semiempirical Design and Estimation Method

The four experimental studies listed in Table 1 have been used to develop the empirical design guidelines for the use of linear theory methods. Each of the studies included wings with differing amounts of camber as determined by the design lift coefficient. The 70-deg arrow wings discussed in the last section are one of the sets of configurations listed in Table 1. The cambered wings of Ref. 15 were designed to develop a uniform load based on the theoretical results of Jones.¹⁶ The wings of Refs. 17 and 18 were designed by the 3-loading optimization method of Ref. 19. The data of Ref. 17 are unique because they show the effect of design lift coefficient at a given Mach number for three different leading-edge sweep angles.

The experimental data and theoretical predictions of WINGDES2 for each wing in Table 1 were used to plot suction parameter at selected values of C_L vs $C_{L,des}$ in the same manner as Fig. 2. As shown in the sketch at the top of Fig. 3, the points of interest are the theoretical and experimental maximum values of suction for a given lift coefficient, $S_{s,max,theory}$ and $S_{s,max,exp}$, and the design lift coefficients, $C_{L,des,opt,theory}$ and $C_{L,des,opt,exp}$, at which they occur. Experimental results in Fig. 3 show that in every case the maximum suction parameter actually achieved was smaller than predicted by theory, and the required surface had less twist and camber (lower $C_{L,des}$) than would be designed by means of linear theory. In addition, these differences become more pronounced with increasing Mach number.

The middle plot of Fig. 3 shows there is essentially a single ratio of $C_{L,des,opt,exp}$ to $C_{L,des,opt,theory}$ for each Mach number. Of particular interest is the data at $M = 2.6$ which have three sweep angles ($\beta \cot \Lambda_{le} = 0.6-0.9$) and still fall along a straight line.¹⁷ This result suggests the use of the design lift coefficient factor

$$K_D = \frac{C_{L,des,opt,exp}}{C_{L,des,opt,theory}}$$

which is shown in Fig. 4. As discussed earlier in regard to Fig. 2, the $C_{L,des,opt,theory}$ can be equated to the C_L for which the wing suction parameter is to be maximized, namely $C_{L,cruise}$. Also the wing lifting surface defined by linear theory which will actually produce maximum performance at $C_{L,cruise}$ is one designed for $C_{L,des} = C_{L,des,opt,exp}$. Thus, the relationship for K_D can be rewritten to define the $C_{L,des}$ for maximum performance at $C_{L,cruise}$ as

$$C_{L,des} = K_D C_{L,cruise} \quad (1)$$

The value of K_D is given in Fig. 4 as a function of Mach number. Since $K_D < 1$, Eq. (1) says that the actual surface always requires less twist and camber (lower $C_{L,des}$) than the theory would indicate. Although this strategy has been used previously in Refs. 13 and 14, e.g., the present study provides a firm basis for the practice and supplies definite quantitative guidelines for its application. An analysis of the 70-deg arrow wing pressure data in Refs. 4 and 5 supports this strategy.

The relationship between the maximum measured suction parameter and the maximum theoretical suction parameter is also shown in Fig. 3. There is somewhat more scatter than in

Table 1 Studies used to define empirical guidelines

Reference	Configuration	M	Λ_{le} , deg	$\beta \cot \Lambda_{le}$	$C_{L,des}$
15	Delta wing body	1.62	68.6	0.49	0, 0.08, 0.20
9	Arrow	2.05	70 deg	0.65	0, 0.08, 0.16
17	Modified arrow wing-body	2.6	69.44	0.90	0, 0.08, 0.12
			72.65	0.75	
			75.96	0.60	
18	Delta wing-body	3.5	76	0.84	0, 0.05, 0.10

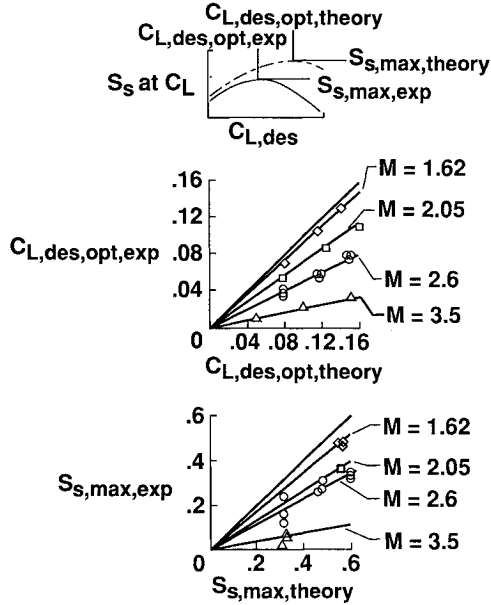


Fig. 3 Optimum design lift coefficient and achievable suction parameter.

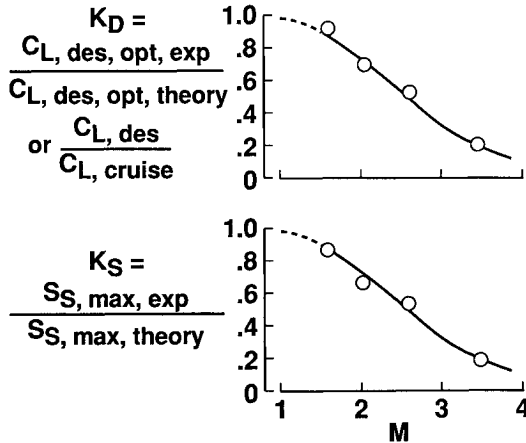


Fig. 4 Empirical factors for selection of optimum design lift coefficient and estimation of achievable suction parameter.

the case of the $C_{L,des}$ plot. The largest scatter, however, occurs for a Mach number of 2.6 at $S_{s,max,theory} = 0.3$ ($\beta \cot \Lambda_{le} = 0.9$). For these wings the bow shock wave is close to the leading edge and would affect the already small level of attainable leading-edge thrust. The results of Fig. 3 were used to define the suction parameter factor

$$K_S = \frac{S_{s,max,exp}}{S_{s,max,theory}}$$

which is also plotted in Fig. 4. Thus, if we call $S_{s,max,exp}$ simply $S_{s,cruise}$, then cruise suction is computed from

$$S_{s,cruise} = K_S S_{s,max,theory} \quad (2)$$

The estimated level of suction from the K_S curve in Fig. 4 is an approximate upper limit of performance achievable with a well-designed lifting surface.^{4,5}

The use of the curves in Fig. 4 for designing a wing for given cruise conditions and estimating its performance may be summarized as follows. First select the cruise lift coefficient and Mach number. Next Fig. 4 is used to obtain the K_D factor and Eq. (1) is used to calculate $C_{L,des}$. A linearized theory computer code is then used to compute the optimum performance surface at $C_{L,des}$ and to obtain the variation of the theoretical suction parameter with C_L . This is the wing surface which will give maximum performance at the cruise conditions. To estimate its performance, Fig. 4 is used to obtain a value for the suction parameter factor K_S . Note that $S_{s,max,theory}$ is essentially the maximum suction parameter for a wing designed for a lift coefficient equal to $C_{L,cruise}$ (not designed for $C_{L,des}$). However, a family of wings designed for different lift coefficients will have approximately the same maximum suction parameter. It is, therefore, sufficient to assume that $S_{s,max,theory}$ is equal to the maximum suction parameter for the wing designed at $C_{L,des}$. Equation (2) can then be used to obtain an estimate of $S_{s,cruise}$.

The drag coefficient at the cruise lift coefficient can be estimated by use of the expression

$$C_{D,cruise} = C_{D,0} + \frac{C_{L,cruise}^2}{\pi AR} + (1 - S_{s,cruise}) \times \left(C_{L,cruise} \tan \frac{C_{L,cruise}}{C_{L,\alpha}} - \frac{C_{L,cruise}^2}{\pi AR} \right) \quad (3)$$

which is derived from the suction parameter definition. The lift-drag polar near the cruise lift coefficient may be approximated by use of a strategy described in Ref. 4.

Although the empirical design and estimation factors were derived from data for wings designed without attainable thrust considerations, they may also be applied to design using the default option of the WINGDES2 code in which camber surface requirements are reduced to a degree consistent with the estimated development of leading-edge thrust. The same tendency for the linearized theory to overestimate the local upwash is present in both cases.

Test Cases for Semiempirical Design and Estimation Method

Existing experimental data were used to assess the validity of the semiempirical design and estimation method. For an existing wing surface, it was first necessary to establish a design lift coefficient by use of WINGDES2 in the evaluation mode. Then the K_D factor was applied to find the cruise lift coefficient for which this surface would have been designed if the empirical design selection method had been used directly. In a certain sense, it is an inverse application of the semiempirical design and estimation method.

The first example shown in Fig. 5 is for the 70-deg arrow wing designed for a lift coefficient of 0.08 at a Mach number of 2 (tested at $M = 2.05$). Because data for this wing (shown in Fig. 1) was included in the derivation of the method, good correlation would be expected and this example does not provide a true test of the method's applicability. It does, however, offer a good example of the use of the method. The key theoretical data as generated by the WINGDES2 code

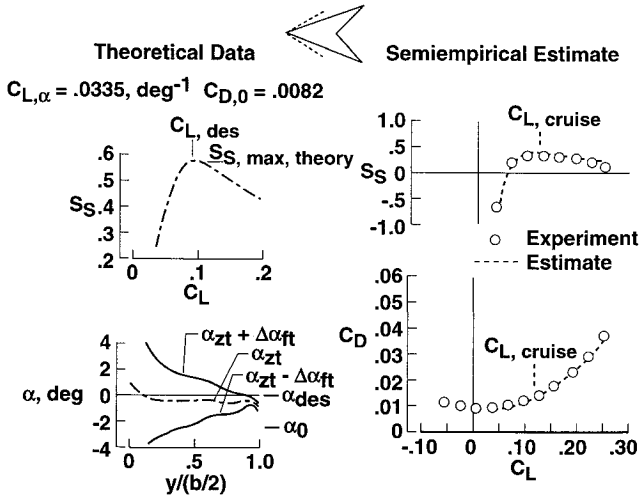


Fig. 5 Application of semiempirical design and estimation method to 70-deg swept arrow wing. $M = 2.05$, $R = 4.4 \times 10^6$.

in its evaluation mode is shown at the left of the figure. The effective design lift coefficient is established by the peak of the suction parameter curve which in this case occurs at a lift coefficient of about 0.085, only slightly different than the original design value. Using a value of $K_D = 0.7$ for a Mach number of 2.05 (Fig. 4), the value of $C_{L, \text{cruise}}$ is found:

$$C_{L, \text{cruise}} = \frac{C_{L, \text{des}}}{K_D} = 0.12$$

In other words, for cruise conditions of a lift coefficient of 0.12 and Mach number of 2.05, the linear theory design lift coefficient is 0.085 and the appropriate linear theory wing design (using a code such as WINGDES2) would have the characteristics shown in Fig. 5. The lower left plot in Fig. 5 illustrates an important criterion in judging how well a particular wing will develop the distributed thrust necessary to recover the theoretical flat wing leading-edge thrust and, therefore, avoid damaging leading-edge flow separation. The development of the distributed thrust requires that the leading-edge slopes of the camber surface be properly matched to the local upwash.⁴ For this discussion it is sufficient to note that the angle-of-attack range for which a cambered wing can develop full leading-edge thrust (i.e., no leading-edge separation) lies between the $\alpha_{zt} + \Delta\alpha_{ft}$ and the $\alpha_{zt} - \Delta\alpha_{ft}$ curves. For a wing whose design angle of attack does not fall within this range, the empirical estimate of performance cannot be made with any assurance of its accuracy due to the development of leading-edge separation. The α_{des} for the 70-deg arrow wing lies well within its range of full leading-edge thrust. This is an indication of a design which recovers the unattainable portion of the theoretical flat-wing leading-edge thrust by the development of a distributed thrust on the forward part of the wing, thereby producing a high level of performance. There is a considerable margin for error in this design since α_{des} lies midway of the range of full leading-edge thrust.⁴

Once the values of K_α , K_D , and the theoretical suction curve are known, Eqs. (2) and (3) can be used to estimate actual suction parameter and drag at the cruise lift coefficient, and the method outlined in Ref. 4 provides an estimate of performance at other lift coefficients near the cruise condition. As seen on the right side of Fig. 5, the estimate shows good agreement with the experimental data. Note that good performance as measured by the suction parameter extends well beyond the $C_{L, \text{cruise}}$ value. The measured suction parameter of about 0.35 for the cruise lift coefficient represents a relatively efficient lifting surface for this Mach number. Full recovery of the theoretical flat wing leading-edge thrust would yield a suction parameter of about 0.55 (Fig. 1).

The remaining examples of application of the semiempirical method are for data not used in the derivation of the method and, therefore, provide a valid test. Data for the arbitrary planform wing body of Ref. 20 is shown in Fig. 6. The wing was twisted and cambered for a lift coefficient of 0.08 at a Mach number of 2.4 using the design methods of Refs. 21–24 with no constraints applied (except upper-surface pressures constrained to values greater than 70% vacuum). This design is more like that produced by the WINGDES2 code in its default mode. The calculated values of $C_{L, \text{des}}$ and $C_{L, \text{cruise}}$ for this case are 0.068 and 0.12, respectively. The α vs span station plot shows that for most of the span the upper limit of full leading-edge thrust matches the design angle of attack α_{des} . The failure to match the full thrust upper limit inboard of 0.1 semispan station and outboard of 0.85 station occurs because the leading edge is supersonic in these regions, and therefore there is no theoretical leading-edge thrust to be attained or recovered. Matching the upper limit of the range of full thrust to the design angle of attack gives a wing with the mildest camber which will maintain attached flow and give performance comparable to a flat wing with full theoretical leading-edge thrust.

As would be expected, the estimation method agrees well with the measured levels of suction and drag. The measured suction parameter at the cruise lift coefficient is about 0.36, while full recovery of the theoretical flat wing leading-edge thrust would yield a suction parameter of about 0.21. Thus, in this case, the twisted and cambered wing has performance appreciably better than the theoretical flat wing. This improvement is due not only to the thrust recovery but also to the development of a wing load distribution which reduced the wave drag due to lift and, perhaps, the vortex drag. Note that above the cruise lift coefficient the suction parameter decreases more rapidly than the previous case. This is a consequence of a design which has the mildest camber surface which will recover the flat wing leading-edge thrust.

Data from Ref. 25 for a 75-deg swept modified arrow wing body are shown in Fig. 7. This configuration was part of a NASA program to develop technology for a supersonic bomber. It is a flying wing concept which was cambered and twisted for a lift coefficient of 0.1 at a Mach number of 3 (a minimum body was used to enclose the model balance). The methods of Refs. 11 and 12 were used to define a lifting surface for an optimum combination of loads. The number of candidate loadings used in the design is not specified and apparently limitations were not placed on the magnitude of the pressure loading (e.g., at the leading edge). At a Mach number of 2.87, the leading edge is swept well behind the Mach line with $\beta \cot \Lambda_{le} = 0.72$. Since flat wing tests were not made, a value of $C_{D,0}$ was computed using the methods of Refs. 21–24.

Photographs of the model in Ref. 25 and the surface numerical description indicate large surface slopes at the wing

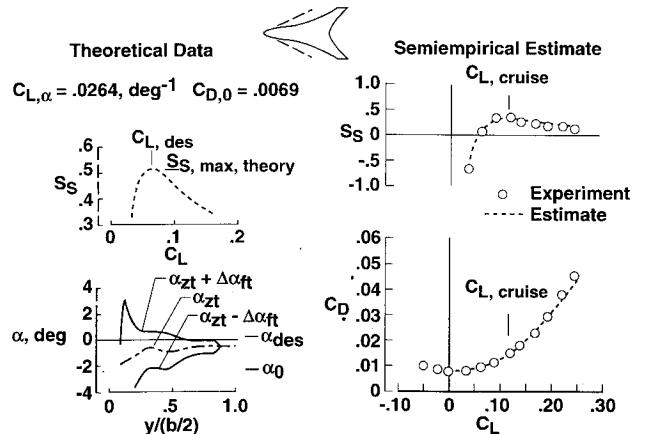


Fig. 6 Application of semiempirical design and estimation method to arbitrary planform wing body. $M = 2.4$, $R = 3.37 \times 10^6$.

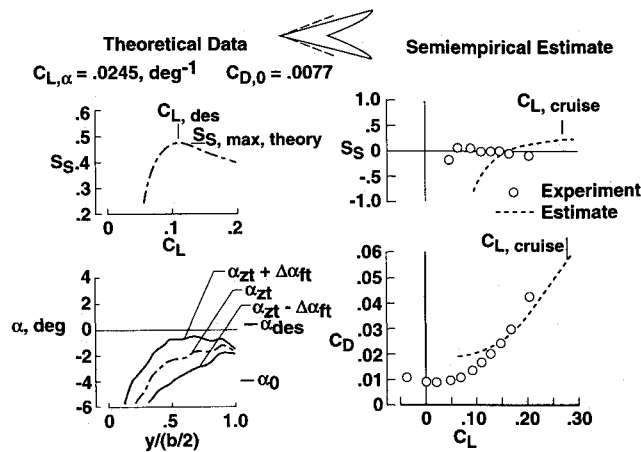


Fig. 7 Application of semiempirical design and estimation method to 75-deg swept modified arrow wing body. $M = 2.87$, $R = 4.2 \times 10^6$.

apex (leading edge up). From a theoretical viewpoint the large slopes at the apex would produce a large amount of lift forward and inboard, which will create a large upwash along the wing leading edge and, therefore, produce high distributed thrust forces in the leading-edge region. However, Fig. 7 shows that performance is far below the level predicted by the semiempirical estimation method. Using the calculated value of $C_{D,0}$, the maximum suction parameter is only slightly larger than zero. Based on observations of data for the other configurations in Ref. 4, it is unlikely that this wing would give aerodynamic performance better than a flat wing. An examination of the WINGDES2 code leading-edge flow conditions shows that this design does not meet the requirements for thrust recovery and avoidance of flow separation and that poor performance would be expected. The large slopes at the apex have produced large negative values of α_{zt} on the inboard region of the wing. As a result, α_{des} is well above the range of full thrust across the entire span and there is, therefore, the probability of flow separation (in fact, an oil-flow photograph in Ref. 25 at $C_L \approx 0.1$ and $M = 2.87$ shows substantial separation). The failure to achieve the performance predicted by the estimation method is not surprising.

Nine additional sample applications of the semiempirical method are given in Ref. 4. Reference 4 also examines the use of an Euler code for estimation of the supersonic performance of twisted and cambered wings and gives a brief review of the linear theory methods for the integration of the wing, fuselage, and nacelles into a complete supersonic cruise aircraft.

Conclusions

A study of the estimation and minimization of drag due to lift at supersonic speeds has yielded the following conclusions:

- 1) Wings with twist and camber, which substitute a distributed thrust over a broad leading-edge region for the concentrated flat wing leading-edge thrust, generally offer better performance than that of the flat wing, but at levels still short of the theoretical potential.
- 2) Comparisons of modified linear theory (WINGDES2 code) and experiment for twisted and cambered wings reveal a consistent qualitative pattern in which the maximum suction parameter actually achieved was smaller than predicted by the theory and the required surface for given flight conditions has less twist and camber than that given by the theory.
- 3) Analysis of data indicates that the employment of a theoretical design lift coefficient less than the desired operational lift coefficient offers an appropriate correction for linearized theory design methods.
- 4) A further analysis of the data led to the development of a semiempirical method for the selection of the proper mod-

ified linear theory design lift coefficient and for the estimation of achievable aerodynamic performance.

5) Application of the semiempirical estimation method to sample cases showed that a reasonable prediction of the measured performance (including the maximum suction parameter and the lift coefficient at which it occurs) was given provided that leading-edge match-up conditions were met.

6) Use of the semiempirical method in conjunction with computer-code data should provide a valuable preliminary design tool for supersonic wing planform tradeoff studies. The modified linearized theory methods require little effort in preparation of input data and can be executed in a relatively short period of time.

References

- ¹Jones, R. T., and Cohen, D., "Aerodynamics of Wings at High Speeds," *Aerodynamic Components of Aircraft at High Speeds*, Vol. VII, *High-Speed Aerodynamics and Jet Propulsion Series*, Princeton Univ. Press, 1957, pp. 3-243.
- ²Chang, I.-C., Torres, F. J., and van Dam, C. P., "Wing Design Code Using Three-Dimensional Euler Equations and Optimization," AIAA Paper 91-3190, Sept. 1991.
- ³Carlson, H. W., and Walkley, K. B., "Numerical Methods and a Computer Program for Subsonic and Supersonic Aerodynamic Design and Analysis of Wings with Attainable Thrust Considerations," NASA CR-3808, Aug. 1984.
- ⁴Carlson, H. W., and Mann, M. J., "Survey and Analysis of Research on Supersonic Drag-Due-to-Lift Minimization with Recommendations for Wing Design," NASA TP-3202, Sept. 1992.
- ⁵Mann, M. J., and Carlson, H. W., "An Assessment of Current Methods for Drag-Due-to-Lift Minimization at Supersonic Speeds," AIAA Paper 91-3302, Sept. 1991.
- ⁶Carlson, H. W., and Mack, R. J., "Estimation of Leading-Edge Thrust for Supersonic Wings of Arbitrary Planform," NASA TP-1270, Oct. 1978.
- ⁷Carlson, H. W., Mack, R. J., and Barger, R. L., "Estimation of Attainable Leading-Edge Thrust for Wings at Subsonic and Supersonic Speeds," NASA TP-1500, Oct. 1979.
- ⁸Polhamus, E. C., "Predictions of Vortex-Lift Characteristics by a Leading-Edge Suction Analogy," *Journal of Aircraft*, Vol. 8, No. 4, 1971, pp. 193-199.
- ⁹Carlson, H. W., "Aerodynamic Characteristics at Mach Number 2.05 of a Series of Highly Swept Arrow Wings Employing Various Degrees of Twist and Camber," NASA TM X-332, Oct. 1960.
- ¹⁰Carlson, H. W., "Pressure Distributions at Mach Number 2.05 on a Series of Highly Swept Arrow Wings Employing Various Degrees of Twist and Camber," NASA TN D-1264, May 1962.
- ¹¹Tucker, W. A., "A Method for the Design of Sweptback Wings Warped to Produce Specific Flight Characteristics at Supersonic Speeds," NACA Rept. 1226, 1955 (supersedes NACA RM L51F08).
- ¹²Grant, F. C., "The Proper Combination of Lift Loadings for Least Drag on a Supersonic Wing," NACA Rept. 1275, 1956 (supersedes NACA TN 3533).
- ¹³Robins, A. W., Morris, O. A., and Harris, R. V., Jr., "Recent Research Results in the Aerodynamics of Supersonic Vehicles," *Journal of Aircraft*, Vol. 3, No. 6, 1966, pp. 573-577.
- ¹⁴Baals, D. D., Robins, A. W., and Harris, R. V., Jr., "Aerodynamic Design Integration of Supersonic Aircraft," *Journal of Aircraft*, Vol. 7, No. 5, 1970, pp. 385-394.
- ¹⁵Brown, C. E., and Hargrave, L. K., "Investigation of Minimum Drag and Maximum Lift-Drag Ratios of Several Wing-Body Combinations Including a Cambered Triangular Wing at Low Reynolds Numbers and at Supersonic Speeds," NACA TN-4020, Sept. 1958 (supersedes NACA RM L51E11, Aug. 1951).
- ¹⁶Jones, R. T., "Estimated Lift-Drag Ratios at Supersonic Speed," NACA TN-1350, July 1947.
- ¹⁷Mack, R. J., "Effects of Leading-Edge Sweep Angle and Design Lift Coefficient on Performance of a Modified Arrow Wing at a Design Mach Number of 2.6," NASA TN D-7753, Dec. 1974.
- ¹⁸Sorrells, R. B., III, and Landrum, E. J., "Theoretical and Experimental Study of Twisted and Cambered Delta Wings Designed for a Mach Number of 3.5," NASA TN D-8247, Aug. 1976.
- ¹⁹Carlson, H. W., and Middleton, W. D., "A Numerical Method for the Design of Camber Surfaces of Supersonic Wings with Arbitrary Planforms," NASA TN D-2341, June 1964.
- ²⁰Darden, C. M., "Effect of Leading-Edge Load Constraints on

the Design and Performance of Supersonic Wings," NASA TP-2446, July 1985.

²¹Middleton, W. D., and Lundry, J. L., "A System for Aerodynamic Design and Analysis of Supersonic Aircraft. Part 1—General Description and Theoretical Development," NASA CR-3351, Dec. 1980.

²²Middleton, W. D., Lundry, J. L., and Coleman, R. G., "A System for Aerodynamic Design and Analysis of Supersonic Aircraft. Part 2—User's Manual," NASA CR-3352, Dec. 1980.

²³Middleton, W. D., Lundry, J. L., and Coleman, R. G., "A

System for Aerodynamic Design and Analysis of Supersonic Aircraft. Part 3—Computer Program Description," NASA CR-3353, Dec. 1980.

²⁴Middleton, W. D., and Lundry, J. L., "A System for Aerodynamic Design and Analysis of Supersonic Aircraft. Part 4—Test Cases," NASA CR-3354, Dec. 1980.

²⁵Hallissy, J. M., and Hasson, D. F., "Aerodynamic Characteristics at Mach Numbers 2.36 and 2.87 of an Airplane Configuration Having a Cambered Arrow Wing with a 75° Swept Leading Edge," NACA RM L58E21, Aug. 1958.

Recommended Reading from Progress in Astronautics and Aeronautics

Applied Computational Aerodynamics

P.A. Henne, editor

Leading industry engineers show applications of modern computational aerodynamics to aircraft design, emphasizing recent studies and developments. Applications treated range from classical airfoil studies to the aerodynamic evaluation of complete aircraft. Contains twenty-five chapters, in eight sections: History; Computational Aerodynamic Schemes; Airfoils, Wings, and Wing Bodies; High-Lift Systems; Propulsion Systems; Rotors; Complex Configurations; Forecast. Includes over 900 references and 650 graphs, illustrations, tables, and charts, plus 42 full-color plates.

1990, 925 pp, illus, Hardback, ISBN 0-930403-69-X

AIAA Members \$69.95, Nonmembers \$103.95

Order #: V-125 (830)

Place your order today! Call 1-800/682-AIAA



American Institute of Aeronautics and Astronautics

Publications Customer Service, 9 Jay Gould Ct., P.O. Box 753, Waldorf, MD 20604
FAX 301/843-0159 Phone 1-800/682-2422 9 a.m. - 5 p.m. Eastern

Sales Tax: CA residents, 8.25%; DC, 6%. For shipping and handling add \$4.75 for 1-4 books (call for rates for higher quantities). Orders under \$100.00 must be prepaid. Foreign orders must be prepaid and include a \$20.00 postal surcharge. Please allow 4 weeks for delivery. Prices are subject to change without notice. Returns will be accepted within 30 days. Non-U.S. residents are responsible for payment of any taxes required by their government.